

An empirical algorithm for determining the diffuse attenuation coefficient K_d in clear and turbid waters from spectral remote sensing reflectance

Tinglu Zhang¹ and Frank Fell^{2*}

¹Ocean Remote Sensing Laboratory of the Ministry of Education of China, Ocean Remote Sensing Institute, Ocean University of China, 5 Yushan Road, Qingdao 266003, China, zhangtl@ouc.edu.cn

²Informus GmbH, Gustav-Meyer-Allee 25, 13355 Berlin, Germany

Abstract

A robust empirical algorithm to determine the diffuse attenuation coefficient K_d at a wavelength of 490 nm (K_d^{490}) from spectral remote sensing reflectance has been derived from the NOMAD data set and tested against the COASTLOOC data set. Together, both data sets contain more than 3,800 observations of concomitantly acquired bio-optical parameters in waters ranging from very clear to very turbid, of which about 2,300 have been used in this study. The proposed algorithm follows a power law of the form $K_d^{490} = 10^{(a_0 + a_1 x + a_2 x^2 + a_3 x^3) + a_4}$ where x is the common logarithm of either of two remote sensing reflectance ratios: $\log_{10}(R_{rs}^{490}/R_{rs}^{555})$ for clear waters and $\log_{10}(R_{rs}^{490}/R_{rs}^{665})$ for turbid waters. Switching between the ratios is triggered when $R_{rs}^{490}/R_{rs}^{555}$ drops below a threshold value of 0.85 corresponding to a K_d^{490} value of approx. 0.2 m^{-1} . Our algorithm shows comparable performance in both clear and turbid waters. Due to its simplicity and the public availability of the underlying in situ data, localization of the algorithm by appropriate sub-setting of the NOMAD data and/or adding other in situ data are straightforward.

Light availability is a critical regulator of physical and bio-geo-chemical processes in the upper ocean layer, such as heating, photosynthesis or species migration to mention just a few (Pennock and Sharp 1986; Lewis et al. 1990; Marra et al. 1995; Bissett et al. 2001; Chang and Dickey 2004). One of the most widely used parameters to describe the availability of light in the water column is the diffuse attenuation coefficient K_d defined as the relative variation of the downward irradiance E_d with depth z :

$$K_d(\lambda, z) = \frac{1}{E_d(\lambda, z)} \frac{dE_d(\lambda, z)}{dz} \quad (1)$$

where E_d and K_d depend on wavelength λ and depth z .

In contrast to the inherent optical properties (IOPs) such as absorption and scattering coefficient, K_d as an apparent optical property (AOP) depends on the angular distribution of light in the water column as well as on inelastic scattering processes such as Raman scattering or chlorophyll fluorescence. K_d therefore, is not constant with depth, even in homogeneous media. However, at the considered wavelength (490 nm) and depth range (first attenuation length, defined as depth where the intensity of E_d has been reduced to $1/e$ of the subsurface value), the contributions of these effects to the downward irradiance and consequently to K_d are small compared to the overall measurement errors and are not considered explicitly in this study.

Due to its importance in global or regional studies, K_d is among the most commonly determined products from spaceborne ocean color measurements. In 1981, Austin and Petzold proposed an algorithm to derive K_d^{490} (i.e., K_d at a wavelength of 490 nm) from atmospherically corrected Coastal Zone Color Scanner (CZCS) measurements using the blue-green ratio of water-leaving radiances L_w :

$$K_d^{490} = K_w^{490} + A \left(\frac{L_w(\lambda_1)}{L_w(\lambda_2)} \right)^B \quad (2)$$

*Corresponding author; Email: fell@informus.de

Acknowledgments

This work was supported by National Natural Science Foundation of China (NSFC) under contract 60378045. The authors would like to express their gratitude to the NASA Ocean Biology Processing Group at Goddard Space Flight Center who compiled the NOMAD data set, as well as to all individual contributors who provided data. The authors also gratefully acknowledge the COASTLOOC project funded by the European Commission under contract ENV-CT96-0310. Special thanks to an anonymous reviewer for a careful review of the preliminary manuscript and to B. Cahill for fine tuning the English.

Table 1. Operational algorithms for $K_d 490$ retrieval for the space-borne instruments.

Sensor	Algorithm	Reference
CZCS*	$k(490) = 0.022 + 0.088 \left[\frac{L_w(443)}{L_w(550)} \right]^{-1.491}$	Austin and Petzold 1981
SeaWiFS†	$k_d(490) = 0.016 + 0.1565 \left[\frac{L_{mw}(490)}{L_{mw}(555)} \right]^{1.540}$	Mueller 2000
MODIS‡	$k_d(490) = 0.016 + 0.1565 \left[\frac{L_{mw}(488)}{L_{mw}(547)} \right]^{1.540}$	Mueller 2000
GLI§	$k_d(490) = 10^{(a_0 + a_1 R + a_2 R^2 + a_3 R^3)}$ $a_i = [-0.825, -1.362, 1.094, -0.777]$ $R = \log_{10} \left(\frac{L_{mw}(460)}{L_{mw}(545)} \right)$	Mitchell and Kahru 1998

*Coastal Zone Color Scanner (CZCS)

†Sea-Viewing Wide Field-of-View Sensor (SeaWiFS)

‡Moderate Resolution Imaging Spectrometer (MODIS)

§Global Imager (GLI)

where $K_w 490 = 0.022 \text{ m}^{-1}$ is the value for the diffuse attenuation coefficient for pure sea water at 490nm as it was known at the time, the reference wavelengths $\lambda_1 = 443 \text{ nm}$ and $\lambda_2 = 550 \text{ nm}$ correspond to the central wavelengths of two CZCS channels, and the coefficients A and B were empirically derived from in situ data (Table 1). Similar algorithms (*see* also Table1) have been developed for the Sea-Viewing Wide Field-of-View Sensor (SeaWiFS) using channels centered at $\lambda_1 = 490 \text{ nm}$ and $\lambda_2 = 555 \text{ nm}$ (Mueller and Trees 1997; Mueller 2000) as well as the Moderate Resolution Imaging Spectrometer (MODIS) using channels centered at $\lambda_1 = 488 \text{ nm}$ and $\lambda_2 = 547 \text{ nm}$ (Mueller 2000). A slightly different approach has been developed by Mitchell and Kahru (1998) for the Global Imager (GLI).

$K_d 490$ algorithms based on blue-green ratios generally work well in clear waters where the optical properties are determined predominantly by the presence of phytoplankton and their degradation products. However, in turbid waters, the uncertainties in the retrieval of $K_d 490$ significantly increase with $K_d 490 > 0.25 \text{ m}^{-1}$ (Mueller 2000). The reason is that turbid waters often are characterized by the presence of inorganic particles showing little correlation with the blue-green ratio.

The unsatisfactory performance of the operational K_d algorithms in turbid waters has led to a search for alternatives. Lee et al. (2005) recently proposed a “semi-analytical” method, i.e., a model-based approach combining theoretical considerations and empirical parameterizations to relate the remote sensing reflectance R_{rs} to K_d via the absorption coefficient a and the backscattering coefficient b_b . In order to improve the performance of their method in turbid waters, they applied a wavelength in the red part of the spectrum. Testing their method on a data set consisting of 875 observations taken in the Gulf of Mexico, the Arabian Sea, and the Baltic Sea, they obtained a significantly higher correlation between $K_d 490$ estimates and measurements within the covered $K_d 490$ range of

0.04 to 4.0 m^{-1} ($R^2 = 0.911$) as compared to the operational SeaWiFS algorithm ($R^2 = 0.680$).

In the present study, we propose a method to determine $K_d 490$ from the spectral R_{rs} of comparable performance to that of Lee et al. (2005). Similar to theirs, our method also uses information in the blue, green, and red part of the spectrum. In contrast to theirs, our method is based entirely on publicly available in situ data and simple statistical evaluation methods. This makes our approach more transparent and more easily adaptable to specific local conditions.

Materials and Procedures

In situ data—Two sets of in situ data are employed in this study: NOMAD (NASA Bio-Optical Marine Algorithm Data Set) and COASTLOOC (Coastal Surveillance through Observation of Ocean Color). In the present study, NOMAD (Werdell and Bailey 2005) is used for algorithm development whereas COASTLOOC (Babin et al. 2003) is applied for algorithm validation. Both data sets contain a multitude of bio-optical parameters, among them concomitantly acquired information on the remote sensing reflectance (NOMAD) or the hemispherical reflectance (COASTLOOC) and the diffuse attenuation coefficient.

NOMAD—The NOMAD data set (Werdell and Bailey 2005) contains more than 3,400 concomitant observations of, among others, the spectral water-leaving radiance $L_w(\lambda)$, the spectral downwelling irradiance on the sea surface $E_s(\lambda)$, and the diffuse downwelling attenuation coefficient $K_d(\lambda)$. NOMAD data have been gathered worldwide between 1991 and 2004 during the course of about 50 different experiments in, optically, very diverse waters with chlorophyll-a ranging between 0.012 mg m^{-3} and 72.12 mg m^{-3} , and $K_d 490$ ranging between 0.016 m^{-1} and 4.6 m^{-1} .

Due to their heterogeneous origin, the radiometric data contained in NOMAD partly differ in their channel setting. However, sufficient information is available to derive a number of simple relationships to shift spectral parameters to the target wavelengths at 490 nm, 555 nm, and 665 nm. In this respect, we have established the following equations (3) to (7).

Equations (3) and (4) are used to shift L_w at 560 nm or 565 nm to the target wavelength 555 nm:

$$L_w 555 = 1.00 [L_w 560]^{0.969} \quad N=441 \quad R^2=0.998 \quad (3)$$

$$L_w 555 = 1.02 [L_w 565]^{0.956} \quad N=802 \quad R^2=0.994 \quad (4)$$

Equations (5) and (6) are used to shift L_w at 625 nm or 670 nm to the target wavelength 665 nm:

$$L_w 665 = 0.674 [L_w 625]^{1.05} \quad N=590 \quad R^2=0.986 \quad (5)$$

$$L_w 665 = 1.04 [L_w 670]^{1.01} \quad N=437 \quad R^2=0.996 \quad (6)$$

Equation (7) is used to relate $E_s 625$ to $E_s 665$:

$$E_s 665 = 1.66 + 0.929 E_s 625 \quad N=558 \quad R^2=0.996 \quad (7)$$

No statistically significant differences are observed between $E_s 555$, $E_s 560$ and $E_s 565$. The same is true for $E_s 665$ and $E_s 670$.

Therefore, E_s560 or E_s565 are used where E_s555 is not available. Similarly, E_s670 is used where E_s665 is not available.

The remote sensing reflectance R_{rs} is obtained as the ratio:

$$R_{rs} = L_w / E_s \quad (8)$$

Using the channel mapping described above, concomitant observations of $R_{rs}490$, $R_{rs}555$, $R_{rs}665$, as well as K_d490 could be made available in 2,248 cases. Of these, eight observations were classified as outliers such that 2,240 NOMAD observations were available for algorithm development.

COASTLOOC—The COASTLOOC data set (Babin et al. 2003) comprises about 420 observations gathered in 1997 and 1998, mostly in European coastal waters. It is entirely independent from NOMAD, i.e., no COASTLOOC data have been integrated into NOMAD so far. COASTLOOC data cover a large variability in terms of water types and constituent concentrations with chlorophyll-a ranging between 0.055 mg m⁻³ and 48.66 mg m⁻³ as well as K_d490 ranging between 0.023 m⁻¹ and 2.83 m⁻¹.

The COASTLOOC data set comprises parameters similar to those contained in the NOMAD data set. Due to the instrumentation employed, the hemispherical reflectance $R(\theta^-)$ just below the sea surface is available instead of the remote sensing reflectance just above surface which is required for the algorithm development in this study. The following Eq. is used to convert between these two parameters (Lee et al. 1994):

$$R_{rs} = \frac{1}{Q} \frac{t^2}{n^2} R(\theta^-) \quad (9)$$

where t is the transmittance of the air-sea interface, n is the real part of the complex refraction index of seawater, and Q designates the upwelling irradiance-to-radiance ratio. All three parameters t , n , and Q depend on a number of external factors such as observation geometry, optical properties of seawater, or wavelength. Of these parameters, Q shows the largest variations under typical measurement conditions, adopting values between ca. 3.5 and 5.0 mainly as a function of water type and solar incidence angle (Loisel and Morel 2001). In this study, t^2/n^2 is approximated by a constant factor of 0.54 (Austin 1974) and Q by a constant factor of 4.0 (Loisel and Morel 2001), resulting in:

$$R_{rs} = 0.133 R(\theta^-) \quad (10)$$

The effects of these approximations, namely on Q , are limited by the fact that remote sensing reflectance ratios are being used subsequently as model variables (see Algorithm development section below) such that much of the dependencies cancel out.

From the 420 COASTLOOC observations, 279 fulfilled the quality criteria and were retained for algorithm validation.

Algorithm development—Operational algorithms to estimate K_d applied by the space agencies are based on various blue-green ratios (Table 1). These algorithms work well in waters where the optical properties are determined predominantly by phytoplankton and their degradation products, but often fail in coastal areas influenced by significant amounts of suspended sediments. In such waters, algorithms based on blue-red ratios are better suited to determine K_d490 . These facts are

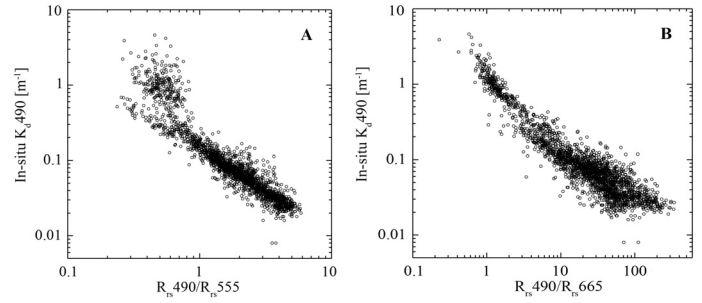


Fig. 1. K_d490 versus remote sensing reflectance ratio for the NOMAD data set. Panel A: K_d490 versus $R_{rs}490/R_{rs}555$; Panel B: K_d490 versus $R_{rs}490/R_{rs}665$.

illustrated in Fig. 1, where the ratios $R_{rs}490/R_{rs}555$ and $R_{rs}490/R_{rs}665$ are depicted against K_d490 for the NOMAD dataset. Whereas the covariance between $R_{rs}490/R_{rs}555$ and K_d490 is high for K_d490 values below ~ 0.2 m⁻¹ (Fig. 1A), exactly the opposite phenomenon is observed for the ratio $R_{rs}490/R_{rs}665$ (Fig. 1B), where higher covariance with K_d490 is observed for K_d490 values above ~ 0.2 m⁻¹.

This observation is the basis for the strategy to develop an improved K_d490 retrieval algorithm. Two independent algorithms shall be applied: one based on the ratio $R_{rs}490/R_{rs}555$ for small values of K_d490 and another based on the ratio $R_{rs}490/R_{rs}665$ for large values of K_d490 . Both algorithms are of the form:

$$K_d490 = 10^{a_{i,0} + a_{i,1} x_1 + a_{i,2} x_1^2 + a_{i,3} x_1^3} + K_w490 \quad (11)$$

where the power law accounts for the dependence of K_d490 on the common logarithm of the color ratio x_i , $i = 1, 2$; $x_1 = \log_{10}(R_{rs}490/R_{rs}555)$, $x_2 = \log_{10}(R_{rs}490/R_{rs}665)$. The constant term K_w490 represents the commonly agreed value ($= 0.016$ m⁻¹) of the diffuse attenuation coefficient for pure sea water.

Two overlapping subsets of in situ data are used to determine the coefficients $a_{i,j}$ in Eq. 11: NOMAD observations of K_d490 where $K_d490 < 0.4$ m⁻¹ are related to $R_{rs}490/R_{rs}555$, whereas NOMAD observations of K_d490 where $K_d490 > 0.1$ m⁻¹ are related to $R_{rs}490/R_{rs}665$. The overlap ensures that both algorithms provide similar results in the K_d490 range between 0.1 m⁻¹ and 0.4 m⁻¹ and reduces edge effects when switching from one algorithm to the other. The coefficients $a_{i,j}$ of Eq. 11 are given in Table 2.

Both algorithms are characterized by a significant error in estimating K_d490 outside their range of applicability (Fig. 2). In order to find a criterion indicating when to switch between the two algorithms, we have applied the following approach: (1) Subdivide the K_d490 range between 0.01 and 10 logarithmically into 30 equidistant intervals; (2) For each interval, determine the performance of either algorithm by calculating the mean relative error of the K_d490 estimate as compared to the direct measurements; (3) Determine the value for K_d490 where the mean relative error functions of the two R_{rs} ratios cross each other; and (4) Determine the R_{rs} ratio corresponding to the identified K_d490 value.

Table 2. Coefficients $a_{i,j}$ of the K_d490 algorithm presented in this article for the K_d color ratios $R_{rs}490/R_{rs}555$ and $R_{rs}490/R_{rs}665$.

Color ratio	Range of validity	$a_{0,j}$	$a_{1,j}$	$a_{2,j}$	$a_{3,j}$
$j = 1: R_{rs}490/R_{rs}555$	$K_d490 < 0.4 \text{ m}^{-1}$	-0.843	-1.459	-0.101	-0.811
$j = 2: R_{rs}490/R_{rs}665$	$K_d490 > 0.1 \text{ m}^{-1}$	0.094	-1.302	0.247	-0.021

Based on the above approach, the following condition (12) has been derived to indicate the switch point between the two R_{rs} ratios:

$$\begin{aligned} \text{if } \{R_{rs}490/R_{rs}555 \geq 0.85\} \text{ use Eq. (11) with } x = \log_{10}(R_{rs}490/R_{rs}555) \\ \text{if } \{R_{rs}490/R_{rs}555 < 0.85\} \text{ use Eq. (11) with } x = \log_{10}(R_{rs}490/R_{rs}665) \end{aligned} \quad (12)$$

Assessment

The performance of our algorithm is assessed in two steps: First, it is investigated in how far the derived algorithm represents the underlying NOMAD dataset. Second, the derived algorithm is applied to the COASTLOOC dataset, which has not been used for the development of the presented algorithm.

Applying the algorithm to the NOMAD dataset gives the results illustrated in Fig. 3A. Estimated and measured K_d490 values are in good agreement for the full range considered. No obvious systematic under- or overestimation is observed. The scatter is rather homogeneous over the full range, including K_d490 values around 0.20 m^{-1} where switching between algorithms takes place. Almost 98% of the estimated K_d490 values are confined within a factor 2.0 error margin, with more than 72% confined within a narrow factor 1.25 error margin. This results in rather small values of the root mean square error (RMSE) on the order of 25%, calculated according to:

$$RMSE = \sqrt{\frac{\sum_{i=1}^N ((K_{d,i}^{der} - K_{d,i}^{mea}) / K_{d,i}^{mea})^2}{N}} \times 100[\%] \quad (13)$$

Additional statistical parameters (R^2 , slope, intercept) have been calculated from log-transformed K_d490 values to equally consider the different orders of magnitude. All three parameters ($R^2 = 0.951$, slope = 0.962, intercept = -0.058) statistically

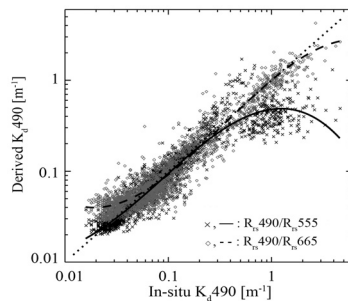


Fig. 2. Derived versus measured values of K_d490 for the NOMAD data set. Polynomial fits underline the fact that the ratio $R_{rs}490/R_{rs}555$ (solid line) is better suited for retrieving K_d490 in clearer waters and $R_{rs}490/R_{rs}665$ (dashed line) is better suited for retrieving K_d490 in turbid waters.

support the visual impression of successful K_d490 retrieval. Further statistical measures are presented in Table 3.

In order to confirm the generic nature of the proposed algorithm, we have applied it to the COASTLOOC dataset. The results are depicted in Fig. 3B. A slight underestimation appears to occur over the full concentration range, most pronounced around $K_d490 = 0.2 \text{ m}^{-1}$. This could be an indication that the switch point between the two algorithms is not ideally suited to the COASTLOOC dataset. However, the overall agreement between estimated and measured K_d490 values is still good ($R^2 = 0.93$), albeit on a slightly lower level statistically. More than 98% of the estimated K_d490 values are confined within a factor 2.0 error margin, with more than 60% confined within a factor 1.25 error margin (Table 4).

A comparison with an operationally applied algorithm has been done by applying the SeaWiFS algorithm to COASTLOOC data. As illustrated in Fig. 4A and supported by the statistical measures presented in Table 4, the SeaWiFS algorithm is of similar performance as our algorithm for K_d490 values below 0.2 m^{-1} . In contrast to that, the SeaWiFS algorithm provides insufficient performance for K_d490 values above 0.2 m^{-1} , as expected from previous studies (Mueller 2000; Lee et al. 2005).

In a further assessment step, we have applied the algorithm of Lee et al. (2005) to the COASTLOOC data (Fig. 4B) where 640 nm was chosen as reference wavelength for application in turbid waters. More than 97% of the Lee et al. estimates of K_d490 are confined within a factor 2.0 error margin, with more than 67% confined within a factor 1.25 error margin. Our algorithm appears to perform better in clear waters ($R^2 = 0.80$ vs. $R^2 = 0.76$), while the Lee et al. algorithm shows a higher correlation between estimates and measurements in turbid waters ($R^2 = 0.79$ vs. $R^2 = 0.86$). Over the full range of K_d490 values, both algorithms show very similar performance ($R^2 = 0.93$ vs. $R^2 = 0.94$).

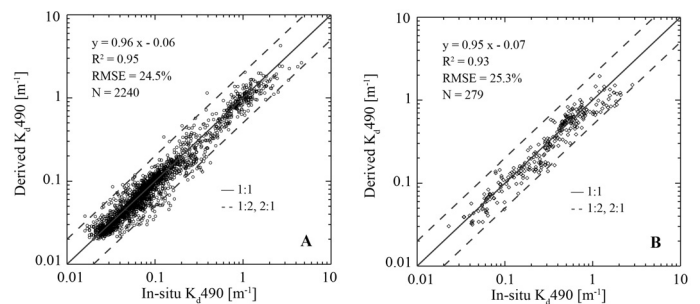


Fig. 3. Application of the K_d490 algorithms developed in this study to the NOMAD (Panel A) and COASTLOOC (Panel B) data sets. Slope, offset and R^2 have been calculated from log-transformed K_d490 values.

Table 3. Representation of the NOMAD dataset by the presented K_d490 algorithm.

K_d490 [m^{-1}]	Statistical measure			
	R^{2*}	RMSE†	F200‡	F125§
≤ 0.2	0.85	23.4	97.9	73.9
> 0.2	0.84	31.0	97.8	62.9
full range	0.95	24.5	97.9	72.1

* R^2 was calculated from log-transformed K_d490 values.
 †RMSE is the root mean square error of the K_d490 estimates in %.
 ‡F200 represents the percentage of K_d490 estimates within a factor 2.0 error margin.
 §F125 represents the percentage of K_d490 estimates within a factor 1.25 error margin.

Discussion

In this study, the NOMAD dataset was used to develop an empirical algorithm for retrieving K_d490 . The algorithm shows comparable performance over a wide range of K_d490 values between $0.02 m^{-1}$ and $2.0 m^{-1}$. It performs better than the algorithms applied operationally to SeaWiFS or MODIS data in turbid waters (where the latter algorithms often fail) and provides a performance similar to the algorithm proposed by Lee et al. (2005). We conclude that our algorithm has significant potential to be operationally applied to Earth Observation data.

When assessing algorithm performance, it should be considered that in situ optical measurements in the ocean are subject to a multitude of error sources of both instrumental origin as well as due to changing external conditions. Even the most careful data processing, including visual inspection and individual treatment of each profile, will not avoid significant error levels. This is especially true for measurements in the red part of the spectrum (as used in this study) where water is highly absorbing and far fewer measurements are available generally within the first optical attenuation length compared to measurements in the blue or green. A significant amount of the observed scatter thus has to be associated to measurement errors of the underlying in situ data.

K_d values are derived from in-water profiles of the downwelling irradiance E_d by applying an exponential fit through the measurements taken within a certain depth interval, mostly the first optical attenuation length. The subsurface upwelling radiance $L_w(O)$ or upwelling irradiance $E_w(O)$ are calculated similarly by fitting an exponential function through

Table 4. Performance of K_d490 algorithms when applied to the COASTLOOC data set.

$[K_d490$ [m^{-1}]	this algorithm				SeaWiFS algorithm				Lee et al. (2005)			
	R^{2*}	RMSE†	F200‡	F125§	R^2	RMSE	F200	F125	R^2	RMSE	F200	F125
≤ 0.2	0.80	23.2	98.9	66.3	0.81	25.3	100.0	70.6	0.76	32.3	95.6	70.6
> 0.2	0.79	26.1	97.9	56.7	0.25	44.0	72.2	22.4	0.86	23.7	98.4	66.6
full range	0.93	25.3	98.2	60.0	0.78	38.6	81.3	38.3	0.94	26.8	97.5	67.6

* R^2 was calculated from log-transformed K_d490 values.
 †RMSE is the root mean square error of the K_d490 estimates in %.
 ‡F200 represents the percentage of K_d490 estimates within a factor 2.0 error margin.
 §F125 represents the percentage of K_d490 estimates within a factor 1.25 error margin.

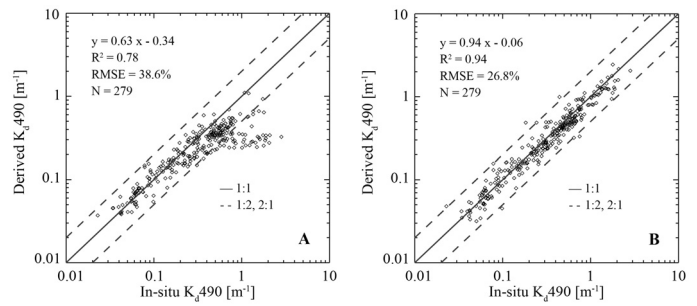


Fig. 4. Application of external K_d490 algorithms to the COASTLOOC data set. Panel A: Operational SeaWiFS algorithm; Panel B: Lee et al. (2005) algorithm. Slope, offset and R^2 have been calculated from log-transformed K_d490 values.

measurements taken in a certain depth interval and subsequent extrapolation to the sea surface. The determination of K_d and especially of $L_w(O)$ or $E_w(O)$ is thus a delicate issue and requires careful visual inspection of every individual profile in order to identify and subsequently exclude problematic measurements influenced by external processes, e.g., wave action, shadowing effects, presence of thin clouds, to name a few.

The proposed method makes use of R_{rs} ratios and, therefore, inherently compensates for some of the errors unavoidably introduced through the atmospheric correction process of space-borne imagery. Better results, nevertheless, are to be expected from airborne or ship-borne measurements where many of the problems from which space-borne measurements often suffer (such as sun glint or atmospheric turbidity) may be avoided.

An important advantage of the method proposed herein lies in the fact that it is entirely based on publicly available and well-documented in situ data, is fully transparent, is easily reproducible, and may be adapted to specific local conditions by sub-setting the underlying data accordingly and/or by adding available data for local areas or specific conditions.

Comments and recommendations

The proposed approach of using two color ratios for determining K_d490 in clear and turbid waters may lead to visual artifacts when applied to satellite imagery. Strictly speaking, such artifacts will be avoided only if the two formulas (Eq. 11) yield the same K_d490 at the switching point. This observation leads to an alternative formulation of the switching criterion: since the two ratios R_{rs490}/R_{rs555} and R_{rs490}/R_{rs665} differ only in their denomi-

nators, this implies that the ratio R_{rs665}/R_{rs555} equals $0.85/5.47 = 0.155$ at the switching point. Due to the functional shape of the two formulas, this alternative switching criterion is unique.

However, the alternative criterion does not intrinsically avoid artifacts when applied to real observations. The coefficients a_0 to a_3 of Eq. 11 for both clear and turbid waters have been derived from more than 2,200 NOMAD observations. If only those measurements taken under specific conditions (e.g., in the Baltic Sea) were to be used for algorithm development, the resulting coefficients would be different and thus lead to other values for either switching criterion. Fortunately, this potential source of image artifacts is, to a large degree, limited by the fact that the algorithms for both clear and turbid waters give very similar results over the K_d490 range between about 0.05 m^{-1} and 0.3 m^{-1} (see Fig. 2).

Looking into the NOMAD data, the implications of this become clear. There are 37 observations in the NOMAD subset used for algorithm development herein taken in conditions near the switching criterion, i.e., where $0.15 < R_{rs665}/R_{rs555} < 0.16$. If the observations were "compliant" to the model developed herein, the derived K_d490 estimates should be close to 0.2 m^{-1} for both the turbid and the clear water algorithm. Whereas this is true for roughly three quarters of the observations ($0.15 \text{ m}^{-1} < K_d490 \text{ derived} < 0.25 \text{ m}^{-1}$ for 21 observations using the clear water algorithm and 29 observations using the turbid water algorithm), data from certain cruises provide significantly different K_d490 estimates (K_d490 ranges from 0.05 m^{-1} to 0.26 m^{-1} for the clear water algorithm and from 0.09 m^{-1} to 0.24 m^{-1} for the turbid water algorithm).

In contrast to that, the differences $\Delta K_d490 = K_d490 \text{ turbid} - K_d490 \text{ clear}$ are small for observations taken close to the switching criterion: of the above mentioned 37 observations, only five showed a difference of $|\Delta K_d490| > 0.03 \text{ m}^{-1}$. Considering the ever present noise in optical measurements, image artifacts should not, therefore, become a problem unless in situations that deviate significantly from the average clear or turbid water conditions represented by NOMAD.

A method to systematically overcome such artifacts is to combine both color ratios within a certain interval around the switching point, using for example an inverse distance weighting approach.

References

- Austin, R. W. 1974. Inherent spectral radiance signatures of the ocean surface, p. 2.1–2.20. *In* Ocean Color Analysis, Scripps Institution of Oceanography, San Diego, CA.
- , and T. Petzold. 1981. The determination of the diffuse attenuation coefficient of sea water using the Coastal Zone Color Scanner, p. 239–256. *In* J. F. R. Gower [ed.], *Oceanography from space*, Plenum Press.
- Babin, M., D. Stramski, G. M. Ferrari, H. Claustre, A. Bricaud, G. Obolensky, and N. Hoepffner. 2003. Variation in the light absorption coefficient of phytoplankton, nonalgal particles and dissolved organic matter in coastal waters around Europe. *J. Geophys. Res.* 108:3211–3230.
- Bissett, W. P., O. Schofield, S. Glenn, J. J. Cullen, W. L. Miller, A. J. Plueddemann, and C. D. Mobley. 2001. Resolving the impacts and feedback of ocean optics on upper ocean ecology. *Oceanography* 14:30–53.
- Chang, G. C., and T. D. Dickey. 2004. Coastal ocean optical influences on solar transmission and radiant heating rate. *J. Geophys. Res.* 109(C01020) [doi:10.1029/2003JC001821].
- Lee, Z. P., K. L. Carder, S. K. Hawes, R. G. Steward, T. G. Peacock, and C. O. Davis. 1994. Model for the interpretation of hyperspectral remote-sensing reflectance. *Appl. Opt.* 33: 5721–5732.
- , M. Darecki, K. L. Carder, C. O. Davis, D. Stramski, and W. J. Rhea. 2005. Diffuse attenuation coefficient of downwelling irradiance: An evaluation of remote sensing methods. *J. Geophys. Res.* 110 (C02017) [doi:10.1029/2004JC002573].
- Lewis, M. R., M. Carr, G. Feldman, W. Esaias, and C. McClain. 1990. Influence of penetrating solar radiation on the heat budget of the equatorial Pacific Ocean, *Nature*. 347:543–545.
- Loisel, H., and A. Morel. 2001. Non-isotropy of the upward radiance field in typical coastal (case 2) waters. *Int. J. Remote Sensing* 22:275–295.
- Marra, J., C. Langdon, and C. A. Knudson. 1995. Primary production, water column changes, and the demise of a Phaeocystis bloom at the Marine Light-Mixed Layers site (59°N, 21°W) in the northeast Atlantic Ocean. *J. Geophys. Res.* 100:6633–6644.
- Mitchell, B. G., and M. Kahru. 1998. Algorithms for SeaWiFS standard products data set. *Cal. Coop. Ocean. Fish. Invest. R.* 39:133–147.
- Mueller, J. L. 2000. SeaWiFS algorithm for the diffuse attenuation coefficient, $K(490)$, using water-leaving radiances at 490 and 555 nm, p. 24–27. *In* S. B. Hooker and E. R. Firestone [eds.], *SeaWiFS postlaunch technical report series, volume 11. SeaWiFS postlaunch calibration and validation analyses, part 3.* NASA Goddard Space Flight Center, Greenbelt, Maryland.
- , and C. C. Trees. 1997. Revised SeaWiFS prelaunch algorithm for the diffuse attenuation coefficient $K(490)$, p. 18–21. *In* S. B. Hooker and E. R. Firestone [eds.], *SeaWiFS technical report series, volume 41. Case studies for SeaWiFS calibration and validation, part 4.* NASA Goddard Space Flight Center, Greenbelt, Maryland.
- Pennock, J. R., and J. H. Sharp. 1986. Phytoplankton production in the Delaware estuary: Temporal and spatial variability. *Mar. Ecol. Prog. Ser.* 34:143–155.
- Platt, T., S. Sathyendranath, C. M. Caverhill, and M. Lewis. 1988. Ocean primary production and available light: Further algorithms for remote sensing, *Deep Sea Res.* 35:855–879.
- Werdell, P. J., and S. W. Bailey. 2005. An improved in situ bio-optical data set for ocean color algorithm development and satellite data product validation. *Remote Sensing of Environment.* 98: 122–140.

Submitted 16 December 2006

Revised 30 August 2007

Accepted 8 September 2007